S/C Band Harmonic Radar for Honey Bee Detection

Fatima Mumtaz, Shobha Sundar Ram and Swapna R. Purandare

Indraprastha Institute of Information Technology Delhi, New Delhi 110020 India
E-mail: {fatima17090, shobha, swapna}@iiitd.ac.in

Abstract—**Harmonic radar technology has been researched and developed for studying the foraging behaviour of honey bees. This work presents the development of a working prototype of a narrow-band harmonic radar system, at 2.5/5GHz, using off-the-shelf components to detect the presence of Indian honey bees. Based on empirical tests on the tag, we estimate the radar probability of detection and probability of false alarms as 88% and 0.3% respectively. The maximum detectable range for a monostatic configuration of the radar is 3.84 m.**

Index Terms—**Harmonic radar, bee detection, harmonic tag**

I. INTRODUCTION

Insect pollinators play a vital role in the functioning of ecosystems. Their foraging behaviour dictates the out-crossing and reproduction of plants by transfer of pollen from male anther to female stigma of flowers [1]. Honey bees are recognized worldwide as one of the most important pollinating agents [2]. Thus the foraging pattern of honey bees is widely studied to understand their behaviour outside the hives which acts as a link to their in-colony activities. Forager bees are divided into scout (less in number) and reticent bees (larger in number). Outside the hives, scout bees are primarily involved in identifying best food resources and transferring the information to reticent bees in the colony. These identified resources are then visited by forager bees for nectar, water, pollen or resin collection [3]. It is of interest to understand which resources are more preferred by a bee species over others, are they visiting the flower beds of same plant species or visiting flower beds of multiple plant species, how much time the bees spent on each flower bed, how far from the hive do they forage, does their foraging behaviour change with experience, do they keep exploring food resources over their lifetime or only in the initial days of their life among others. These questions can be answered by tracking bees over their entire lifespan [4]. The answers can help scientists understand the reason for the waning population of bees and agriculturists to strategize plant cultivation. Thus developing technology to help assist tracking the path of bees over their lifetime is crucial.

Many field studies have utilized the radio frequency identification (RFID) technology to count the number of trips made by bees [5]–[9]. A passive RFID tag attached to the bee allows the RFID readers installed at the entrance of the hive to detect the bee whenever it enters or leaves the hive, allowing to keep count of the trips completed in a day. However, current RFID technology does not have the ability to perform localization of bees since they have very small working range of the order of a few millimeters. Moreover, entrance and exit paths to the hives need to be defined for the bees, disturbing the natural habitat of the species.

Traditional radar has failed to track bees due to the low radar cross-section of the insect caused by its small size. As a result, the scattered signals from the radar are very weak and well below the noise floors of most radar receivers. Also, high ground clutter mask weak signals from targets. Harmonic radars are an alternative to the conventional radar and are used to detect and track cooperative targets. Here, a radar transmits a signal at a fundamental frequency. A passive harmonic tag is attached to a target insect, where harmonics of the received radar signal are generated. The radar receiver is tuned to receive one of the higher order harmonics, usually the second order harmonic. The received signal strength is thus a function of the electrical characteristics of the tag rather than the physical size of the insect. Hence, the tag can be carefully designed so as to enable the detection of the insect even in the presence of noise and clutter. To ensure monitoring of bees over their lifetime, it is important to design a tag carefully so as to not cause any hindrance to its movements and day to day activities. The tag must not rely on a perishable power source. The application of harmonic radar technology to track bees was first proposed in [10]. The radar consisted of a 9.4 GHz transmit frequency and 18.8GHz receive frequency and 16 mm long lightweight tag comprising of a dipole, a diode and an inductive loop as detailed in [10], [11]. The harmonic radar has been successfully utilized in many field studies [4], [12]–[16]. It was observed that the tag does not seem to cause any abnormality in the foraging behaviour of the bee [17]. Many harmonic tag designs operating at different operating frequencies have been proposed. The tag designs explored different types of tag antennas including both wire and patch antennas [18], [19]. However, the dipole transponder is the most widely used tag design for field studies.

Most of the field studies have been carried out to track the *Apis mellifera*, a European honey bee species. We aim to study the foraging behaviour of Indian honey bee, *Apis dorsata dorsata*. In this paper we present a narrowband 2.5GHz/5GHz harmonic radar developed in our institute premises for tracking the foraging behavior of Indian honey bees. The choice of these frequencies is guided by the ubiquity of hardware resources due to the popularity of these bands for WiFi and other wireless communication applications. Our paper is organized in the following manner. In the following section, we introduce the principles of the harmonic radar. In Section.III, we describe the design and fabrication of our radar and in Section.IV, we present the detection performance of our radar.

II. INTRODUCTION TO HARMONIC RADAR

Let $P_{tx}^{f_0}$ be the power transmitted by the narrowband transmitter of a harmonic radar located at the origin with a directional antenna of gain $G_{tx}^{f_0}(\theta, \phi)$ at frequency f_0. The electromagnetic signal impinges on a cooperative target that carries a harmonic tag. The simplest configuration of a harmonic tag consists of an antenna (usually a dipole) and a diode. The power density impinging upon a harmonic tag placed at (R, θ, ϕ) from the radar is given by

$$S_{tx}^{f_0} = \frac{P_{tx}^{f_0} G_{tx}^{f_0}(\theta, \phi)}{4\pi R^2} \tag{1}$$

For λ_0 wavelength, the effective receive area $A_{tag}^{f_0}$ of the tag is

$$A_{tag}^{f_0} = \frac{\lambda_0^2 G_{tag}^{f_0}(\theta, \phi)}{4\pi}. \tag{2}$$

Then the amount of power absorbed by the tag's antenna, $P_{tag}^{f_0}$, is given by

$$P_{tag}^{f_0} = \frac{P_{tx}^{f_0} G_{tx}^{f_0}(\theta, \phi) A_{tag}^{f_0}}{4\pi R^2}. \qquad (3)$$

A portion of the captured power passes through the non-linear diode giving rise to a voltage, $v_{diode}(t)$, at f_0. The diode current, i_{diode}, according to the Schockley diode equation is

$$i_{diode}(t) = I_s(e^{\alpha v_{diode}(t)} - 1) \qquad (4)$$

where I_s is the reverse bias saturation current, $\alpha = \frac{q}{nkT}$, q is the electronic charge ($1.6 \times 10^{-19} C$), n is the emission coefficient of the diode, k is the Boltzmann constant and T is the absolute temperature ($\sim 290K$). Due to the non-linear nature of the current-voltage relationship of a diode, harmonics of f_0 are generated and re-radiated by the antenna as shown in

$$P_{tag} = \sum_{n=1}^{\infty} P_{tag}^{nf_0} = \sum_{n=1}^{\infty} d_n(P_{tag}^{f_0})^n \qquad (5)$$

where d_n is the scaling factor corresponding to the nth harmonic with units $\frac{1}{W^{n-1}}$. The power density reflected back to the radar at distance R by the tag at n^{th} harmonic is proportional to the gain of the tag at nf_0

$$S_{rx}^{nf_0} = \frac{P_{tag}^{nf_0} G_{tag}^{nf_0}(\theta, \phi)}{4\pi R^2} \qquad (6)$$

The radar receiver is tuned to receive the higher order harmonic. The received power at the radar is

$$P_{rx}^{nf_0} = S_{rx}^{nf_0} G_{rx}^{nf_0}(\theta, \phi) \frac{\lambda_0^2}{4\pi n^2} \qquad (7)$$

where $G_{rx}^{nf_0}(\theta, \phi)$ is the gain of the radar receiving antenna at nf_0. Expanding the above equation we get the generalized form of the non-linear radar range equation,

$$P_{rx}^{nf_0} = \left[\left(P_{tx}^{f_0} G_{tx}^{f_0}(\theta, \phi) \right)^n G_{rx}^{nf_0}(\theta, \phi) \right] \left[G_{tag}^{nf_0} d_n (A_{tag}^{f_0})^n \right] \\ \left[\frac{\lambda_0^2}{n^2 (4\pi)^{n+2} R^{2n+2}} \right]. \qquad (8)$$

The first set of terms in (8) are related to the radar system parameters such as the gain of the transmitting and receiving antennas and the transmitted power. The second set of terms correspond to the tag parameters while the third set of terms correspond to the free space loss. Equation (8) reduces to the well known Frii's radar range equation when $n = 1$ corresponding to linear radars.

$$P_{rx}^{f_0} = \left[P_{tx}^{f_0} G_{tx}^{f_0}(\theta, \phi) G_{rx}^{f_0}(\theta, \phi) \right] \left[\sigma^{f_0} \right] \left[\frac{\lambda_0^2}{(4\pi)^3 R^4} \right] \qquad (9)$$

where σ^{f_0} is the linear radar cross-section of the target that indicates the amount of signal returned by the target to the radar. Mathematically, σ^{f_0} is defined as [20]

$$\sigma^{f_0} = 4\pi \frac{P_{rx}^{f_0}}{S_{tx}^{f_0}}, \qquad (10)$$

and is a function of the shape, material, physical area and aspect angle of the target and polarization and frequency of the transmitted signal. In the case of the harmonic radar, the RCS σ^{nf_0} is given by

$$\sigma^{nf_0} = 4\pi \frac{P_{rx}^{nf_0}}{S_{tx}^{f_0}} = d_n G_{tag}^{nf_0}(\theta, \phi)(A_{tag}^{f_0})^n. \qquad (11)$$

Thus the harmonic radar cross-section is a function of the electrical properties of the tag such as the gain of the antenna and the non-linearity inherent in the diode. Therefore the harmonic radar is usually used only in situations where $\sigma^{nf_0} > \sigma^{f_0}$. This usually corresponds to situations where the target's linear radar cross-section is very low such as insects.

III. DESIGN METHODOLOGY

Our design methodology was guided by the philosophy of using cheap, off-the-shelf components and available laboratory resources.
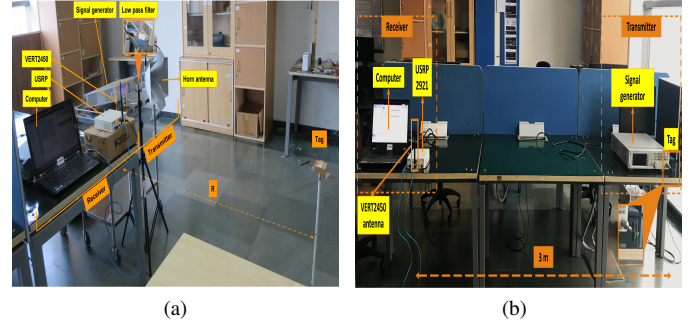

(a)   (b)

Fig. 1. (a) Monostatic configuration of harmonic radar with two-way path loss. (b) Experimental setup for verification of one-way path loss from tag to harmonic radar receiver.

Our harmonic radar, shown in Fig.1(a), is designed to operate at 2.5GHz transmitting frequency and 5GHz receiving frequency.

A. Hardware description of the transmitter and receiver

Agilent N5181A MXG analog signal generator is used to generate a continuous wave sinusoidal signal at 2.5GHz with a maximum signal power of 30dBm. The harmonic radar detection performance is susceptible to clutter from harmonics generated by the transmitting oscillator at high power. Therefore, we pass the generated signal through a customized microstrip low pass filter with a cut-off frequency at 3GHz. We implemented the filter on an FR4 substrate (relative permittivity = 4.7, thickness of dielectric = 1.5mm, copper thickness = 35um).

The signal from the low pass filter is radiated via a broadband R&S HF907 double rigid wave guide horn antenna of 8.91dBi gain at 2.5GHz. The signal from the tag is picked by the receiving horn antenna. It is imperative for the receiver to reject signals at 2.5GHz since they may give rise to higher order harmonics at the later amplification stages in the receiver chain. The two main sources of the fundamental frequency at the receiver are: (1) the direct signal from the transmitter (2) the reflected signal from the tag at the fundamental frequency. To overcome this issue, we use a custom designed microstrip coupled line band pass filter to block the fundamental frequency signals from entering the receiver chain while allowing second harmonic signal to pass through. The filter is designed on a Rogers RO4003C (relative permittivity = 3.38, thickness of dielectric = 0.813mm, copper thickness = 35um) substrate. The filters were enclosed in an aluminum box to shield them from radio frequency interference and for making the design sturdy to handle the pressure from the RF cables and connectors. Please note that the band pass filter introduces a loss of -6.63dB. Hence, the use of the filter trades off between suppression of the fundamental frequency and the signal attenuation at 5GHz. To measure the received signal, we used NI USRP-2921, a software defined radio module, which is a tunable half-duplex RF transceiver. The device can receive signals in either the frequency range of 2.4-2.5GHz or 4.9-5.9GHz. Therefore, the receiver can be configured as a traditional radar or as a harmonic radar and their performances can be compared. The gain of the low noise amplifier was set at 10dB. We implemented receiver configuration with an intermediate frequency at 40KHz in order to mitigate the effects of flicker noise in the circuitry. We selected a sampling frequency of 100KHz to save the time-domain signal which is was time averaged to achieve a noise floor of -108dBm. The USRP streams baseband in-phase and quadrature signals to host computer over a 1 Gigabit Ethernet.

B. Components of the Harmonic Tag

The harmonic tag consists of three components: a wire dipole antenna, a diode and an inductive loop. The wire dipole antenna acts as a half-wave dipole receiver at 2.5GHz and a full-wave dipole transmitter at 5GHz. The advantage of using this antenna design is four-fold. Firstly, utilizing the same antenna for transmission and reception saves up on the the size of the tag. Secondly, the vertically standing structure of a wire dipole is advantageous for small insect targets as it can be mounted on a very small area on the insect body causing minimal interference with the legs and wings. Thirdly, the dipole has an omnidirectional radiation pattern which would enable the detection of the insect along different orientations. Lastly, the dipole has a fat doughnut shaped directivity pattern making it less susceptible to large fluctuations in performance with small antenna tilts. The fabricated dipole is 60mm in length. The wire used is an uninsulated copper wire of 0.5mm thickness. The dipole antenna transfers the received signal at f_0 to the diode attached to its feed point. The signal triggers the diode to produce the diode current that contains the incident frequency (f_0) and the harmonics of the incident signal frequency because of its non-linear property. We considered four off-the-shelf diodes for our design - SMS7630-079LF, BAT15-03W, HSMS-286K-BLKG and SMV1249-079LF. All these four diodes are rated to work at the desired radar frequencies. The first three are Schottky diodes while the last one is a junction tuning varactor diode.

In order to improve the efficiency of the tag, we incorporate an inductive loop across the diode. The inductive loop performs two major functions: (1) The loop acts as a direct current path allowing the flow of accumulated electrostatic charges thereby enabling the diode to operate in the zero-bias mode [19], (2) the loop helps in impedance matching the dipole with the diode to improve the efficiency of the overall tag performance. A laboratory experiment was conducted to check the performance of the tag for different inductance values. Similar tags were fabricated for all four diodes mentioned above. The experiment uses the one-way transmission set-up shown in Fig.1(b). The power transmitted by the signal generator was varied and the received power are presented in Fig.2(a)-(d) while Fig.2(e) shows a set of tags fabricated for different loop dimensions. From the experiment, the following observations are made: Figure 2(a) shows the performance of SMS7630-079LF diode. It is seen that the tags with 5.3nH and 7nH loops have comparable performance. Increasing the loop inductance degrades the performance of the tag. Figure 2(b) shows the performance of BAT15-03W diode. It performs well for 5.3nH loop. The performance deteriorates for other inductance values. Figure 2(c) shows the performance of SMV1249-079LF diode. The tag is not detectable at transmitted power levels up to 15 dBm with or without the loop. Figure 2(d) shows the performance of HSMS-286K-BLKG diode. Though the tag performs well at high power levels, the received power is very low when the transmitted power level is below -10dBm. This is due to the low junction capacitance associated with the varactor diode leading to significant impedance mismatch. Based on the above experiments, we shortlisted the SMS7630-079LF and BAT15-03W diodes and inductive loop of 5.3nH for fabrication of tag for further experiments.

IV. EXPERIMENTAL RESULTS

In this section, we test the performance of the harmonic radar system and tag that were developed. First, we determine the maximum detectable range of a monostatic radar configuration using the experimental set up shown in Fig. 1(a). The tag was mounted on a stand that was moved away from the radar, along the radial direction
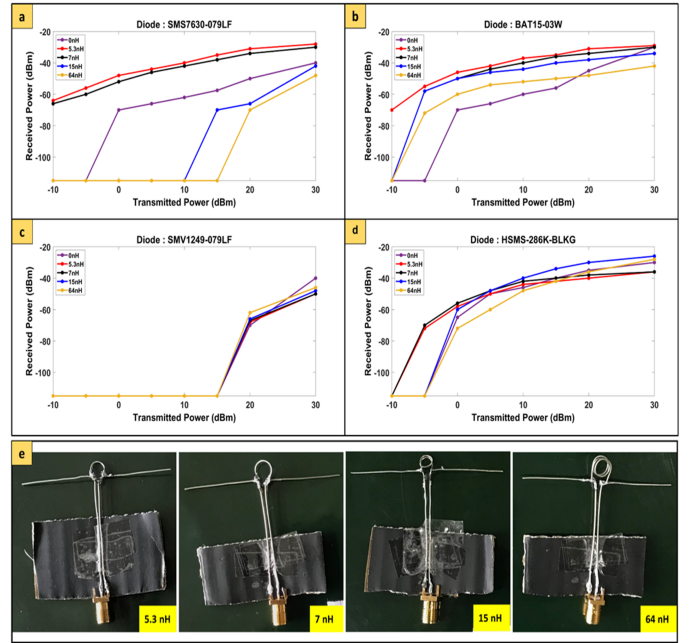

Fig. 2. The received power versus the transmitted power for different inductor-diode combinations. The diodes are (a)SMS7630-079LF, (b)BAT15-03W, (c)SMV1249-079LF and (d)HSMS-286K-BLKG respectively. (e) Photograph of a set of fabricated harmonic tags for SMS7630-079LF diode for different values of inductance of the loop. The inductance values of the loop for each tag is mentioned on the bottom right corner of each tag.

until the received signal was below the noise floor (at -106dBm) and hence not detectable. The maximum detectable range was recorded as 3.84m.

Since the two-way propagation path loss is high for monostatic configuration resulting in low coverage area for detection of targets, we conducted a study to check whether there is an improvement in the performance by implementing a bistatic configuration as shown in Fig.3(b). The transmitter horn is placed at [2.9m, 1m, 1.1m] while the receiver horn is placed at [1m, -0.8m, 1.1m]. For the study, we selected a controlled space to monitor the activities of bees. We chose to use a double bed folding mosquito net shown in Fig.3(a). The net is cheap, introduces zero attenuation, easy to assemble and disassemble and has the required dimensions for easy movement of bees. We measured the received power at the radar by placing the tag at 29 points at different positions and heights within the net. The recorded results are presented visually on the top view of the net. The solid lines of varying thicknesses in the figure depict contour lines at different heights. For example, the outermost contour depicts a height of h_1=0.2m. Fig. 3(b) shows the amount of power received. The color of the dots indicate the range of the strength of the received power (in dBm). The figure shows that the radar is able to detect the target at most of the positions except for the corners.

A. Detection performance

Next, we evaluated the probability of detection and false alarm for the system using Monte Carlo simulations. We modeled the transmitted power $P_{tx}^{f_0}$ as 30 dBm for $f_0 = 2.5GHz$. We modeled the position coordinates of the tag as a random three dimensional vector that could lie anywhere within a cuboid of dimensions comparable to the net ($2m \times 2m \times 1.4m$) with uniform probability. The transmitting and receiving antenna were modeled at positions $[2.9 \times 1m \times 1.1m]$ and $[1m \times -0.8m \times 1.1m]$. If $R_{tx \to tag}$ is the
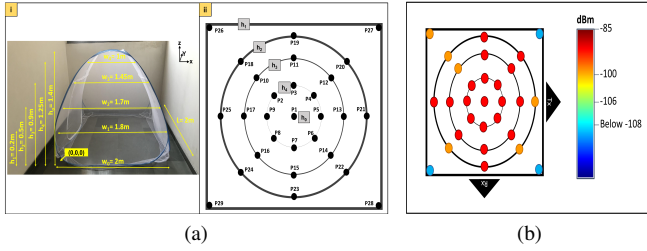
Fig. 3. (a) Bistatic radar configuration to detect tag within region of interest showing (i) dimensions of the region(net) (ii) marked positions for measurements, (b) detected power in dBm.
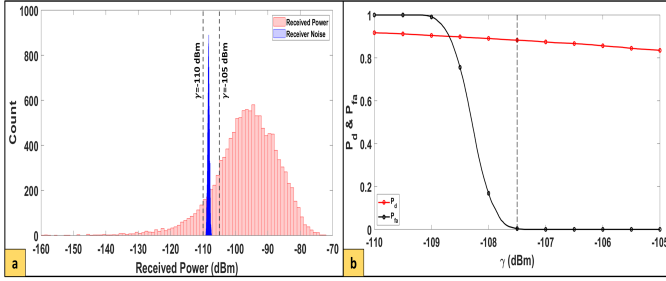

Fig. 4. (a) Histogram plot of the receiver power and noise level of the radar system (b) Plot of probability of detection (P_d) and probability of false alarm (P_{fa}) as a function of threshold (γ) varying from -110dBm to -105dBm

distance of the tag from the transmitter and $R_{tag \to rx}$ is the distance of the tag from the receiver, then the received power at $2f_0$ can be calculated by suitable modification from monostatic to bistatic configuration of the harmonic radar range equation presented earlier. Note that the gains of the the radar and the tag antennas vary with the azimuth and elevation aspect of the tag with respect to the radar. The non-linear radar cross section was modelled as a random variable with a Gaussian distribution ($N(0, 2.46)$) to incorporate the variations due to the tilt of the tag. The value of d_2 (the harmonic second order power coefficient) was taken to be 0.2 from simulation studies of the chosen diode. Cable losses (L) of 3dB were measured. Once the received power was simulated, we added white Gaussian noise of $N(0, 0.0914)$. The histogram of the received signal and noise was simulated in MATLAB for 12412 Monte Carlo trials and presented in Fig. 4(a). The receiver noise characteristics were estimated from the noise floor of the USRP at 5 GHz by running the receiver hardware without switching on the transmitter. The noise histogram is also plotted in the figure. The probability of detection (P_d) is given by the area under the histogram of the received signal and noise power above a pre-defined threshold (γ). The probability of false alarm (P_{fa}) is the area under the histogram of the noise power above the same threshold. The P_{fa} and P_d are plotted as a function of γ in Fig.4(b). Based on the figure, the value of γ is selected as -107.5dBm to reduce the probability of false alarm to 0.3% while maximizing probability of detection to 88.3%.

V. Conclusion

We demonstrated a working prototype of a narrowband harmonic radar, developed using off-the-shelf components, that operates at 2.5GHz transmit and 5GHz receive frequency. The maximum detectable range of the developed radar was 3.84 m for a monostatic configuration. Empirical tests determined a probability of detection of 88.3% and probability of false alarm of 0.3% for a signal threshold of -107.5dBm under bistatic configuration.

References

[1] C. Eardley, D. Roth, J. Clarke, S. Buchmann, B. Gemmill *et al.*, *Pollinators and pollination: a resource book for policy and practice.* Agricultural Research Council (ARC), 2006.

[2] M. Aizen and P. Feinsinger, "Bees not to be? responses of insect pollinator faunas and flower pollination to habitat fragmentation," in *How landscapes change.* Springer, 2003, pp. 111–129.

[3] H. Abou-Shaara, "The foraging behaviour of honey bees, apis mellifera: a review." *Veterinarni medicina*, vol. 59, no. 1, 2014.

[4] J. L. Woodgate, J. C. Makinson, K. S. Lim, A. M. Reynolds, and L. Chittka, "Life-long radar tracking of bumblebees," *PloS one*, vol. 11, no. 8, p. e0160333, 2016.

[5] S. Klein, C. Pasquaretta, X. J. He, C. Perry, E. Søvik, J.-M. Devaud, A. B. Barron, and M. Lihoreau, "Honey bees increase their foraging performance and frequency of pollen trips through experience," *Scientific reports*, vol. 9, no. 1, p. 6778, 2019.

[6] C. W. Schneider, J. Tautz, B. Grünewald, and S. Fuchs, "Rfid tracking of sublethal effects of two neonicotinoid insecticides on the foraging behavior of apis mellifera," *PloS one*, vol. 7, no. 1, p. e30023, 2012.

[7] A. Decourtye, J. Devillers, P. Aupinel, F. Brun, C. Bagnis, J. Fourrier, and M. Gauthier, "Honeybee tracking with microchips: a new methodology to measure the effects of pesticides," *Ecotoxicology*, vol. 20, no. 2, pp. 429–437, 2011.

[8] D. F. Minahan and J. Brunet, "Strong interspecific differences in foraging effort observed between honey bees and bumble bees using miniaturized radio frequency identification (rfid)." *Frontiers in Ecology and Evolution*, vol. 6, p. 156, 2018.

[9] P. Nunes-Silva, M. Hrncir, J. Guimarães, H. Arruda, L. Costa, G. Pessin, J. Siqueira, P. De Souza, and V. Imperatriz-Fonseca, "Applications of rfid technology on the study of bees," *Insectes sociaux*, vol. 66, no. 1, pp. 15–24, 2019.

[10] J. Riley, A. Smith, D. Reynolds, A. Edwards, J. Osborne, I. Williams, N. Carreck, and G. Poppy, "Tracking bees with harmonic radar," *Nature*, vol. 379, no. 6560, p. 29, 1996.

[11] J. Riley and A. Smith, "Design considerations for an harmonic radar to investigate the flight of insects at low altitude," *Computers and Electronics in Agriculture*, vol. 35, no. 2-3, pp. 151–169, 2002.

[12] D. Milanesio, M. Saccani, R. Maggiora, D. Laurino, and M. Porporato, "Recent upgrades of the harmonic radar for the tracking of the asian yellow-legged hornet," *Ecology and evolution*, vol. 7, no. 13, pp. 4599–4606, 2017.

[13] S. Wolf, D. P. McMahon, K. S. Lim, C. D. Pull, S. J. Clark, R. J. Paxton, and J. L. Osborne, "So near and yet so far: harmonic radar reveals reduced homing ability of nosema infected honeybees," *Plos one*, vol. 9, no. 8, p. e103989, 2014.

[14] E. A. Capaldi, A. D. Smith, J. L. Osborne, S. E. Fahrbach, S. M. Farris, D. R. Reynolds, A. S. Edwards, A. Martin, G. E. Robinson, G. M. Poppy *et al.*, "Ontogeny of orientation flight in the honeybee revealed by harmonic radar," *Nature*, vol. 403, no. 6769, p. 537, 2000.

[15] D. W. Williams, G. Li, and R. Gao, "Tracking movements of individual anoplophora glabripennis (coleoptera: Cerambycidae) adults: application of harmonic radar," *Environmental entomology*, vol. 33, no. 3, pp. 644–649, 2004.

[16] J. C. Makinson, J. L. Woodgate, A. Reynolds, E. A. Capaldi, C. J. Perry, and L. Chittka, "Harmonic radar tracking reveals random dispersal pattern of bumblebee (bombus terrestris) queens after hibernation," *Scientific reports*, vol. 9, no. 1, p. 4651, 2019.

[17] N. Carreck, "The use of harmonic radar to track flying bees," *Bee Craft (United Kingdom)*, 1996.

[18] K. Rasilainen and V. V. Viikari, "Transponder designs for harmonic radar applications," *International Journal of Antennas and Propagation*, vol. 2015, 2015.

[19] R. Brazee, E. Miller, M. Reding, M. Klein, B. Nudd, and H. Zhu, "A transponder for harmonic radar tracking of the black vine weevil in behavioral research," *Transactions of the ASAE*, vol. 48, no. 2, pp. 831–838, 2005.

[20] I. S. Merrill *et al.*, "Introduction to radar systems," *Mc Grow-Hill*, vol. 7, no. 10, 2001.